Evaluation of the coefficient of subgrade reaction for design of multi-propped diaphragm walls from DMT moduli

P. Monaco & S. Marchetti
University of L'Aquila, Italy

Keywords: diaphragm walls, subgrade reaction method, flat dilatometer test

ABSTRACT: This paper presents the preliminary results of a numerical study on multi-propped walls retaining deep excavations. The study is based on the comparison between the results obtained by FEM (Plaxis) using the non linear Hardening Soil model and by the Subgrade Reaction Method, considering different wall / soil stiffness, excavation depth and prop spacing conditions. A tentative relation, "calibrated" vs FEM results, is proposed for deriving the coefficient of subgrade reaction Kh for design of multi-propped diaphragm walls from the constrained modulus M from DMT.

1 INTRODUCTION

Multi-propped or multi-anchored diaphragm walls are widely used today for retaining deep open pit excavations in urban areas (e.g. underground car parkings), often in combination with the "top-down" construction technique, in order to limit the deformations in the surrounding soil.

The design of multi-restrained retaining walls requires the use of methods of analysis which take into account the soil-structure interaction and permit to simulate the staged construction sequence. Though the Finite Element Method (FEM) approach is generally regarded today as the "way to the future", in common practice the simple and well-known Subgrade Reaction Method (SRM) or "spring method" is still widely used and often preferred to more sophisticated FEM analyses, particularly in the early stage of design. The SRM permits to model even relatively complex cases in a simple and quick way, providing in general sufficiently reliable values of stresses in the wall and supports. On the other hand the SRM has several drawbacks, deriving from the rough simplification assumed in simulating the response of the soil to wall movements. One critical shortcoming is the difficulty in evaluating the coefficient of subgrade reaction K_h on a rational base. K_h is by no means an intrinsic property of the soil. Its value depends not only on soil stiffness, but also on various "geometric-mechanical" factors (e.g. geometry and stiffness of wall/struts, excavation depth). Yet the influence of the above factors on K_h is not clearly understood. Hence indications for the selection of K_h values dependable for design may be helpful to

many engineers who still rely on the "old" SRM for everyday practice.

This paper presents the preliminary results of a numerical study aimed at establishing tentative correlations for deriving K_h for design of multi-propped diaphragm walls from the constrained modulus M_{DMT} obtained from the flat dilatometer test (Marchetti 1980). Comparisons both in terms of M_{DMT} vs "reference" M and in terms of predicted vs measured settlements (see reference list in TC16 2001) have shown that, in general, M_{DMT} is a reasonably accurate "operative" modulus.

The study is based on the comparison between FEM and SRM results, according to the following procedure: (1) Analysis of the behavior of a multi-propped wall for various cases by FEM (Plaxis) using the non linear Hardening Soil model, with soil stiffness parameters estimated from M_{DMT}. (2) Analysis by SRM varying K_h until the results obtained by Plaxis for the same cases are appropriately reproduced. (3) Formulation of a tentative relation between backcalculated "best fit" K_h values (matching FEM results) and M_{DMT}.

The study is purely numerical. K_h values are "calibrated" based on FEM results, assumed herein to represent the "true" wall / soil behavior. No comparisons are shown between the behavior predicted by the models and observed in real cases.

2 SPRING MODEL VS CONTINUUM

In the spring model the soil is schematized by a set of independent horizontal springs, generally characterized by a bilinear elastic-plastic pressure-

displacement relation (Fig. 1). The coefficient of subgrade reaction Kh (spring stiffness) is the initial slope of the curve until the limit pressure, active or passive, is reached. Hence a purely 2-D (plane strain) problem is converted into a 1-D problem. The soil behavior is "captured" by only one parameter, Kh. The simplest case of homogeneous isotropic linear elastic continuum requires a minimum of two parameters (E and ν, or G and K) to fully define it.

In general, it is not possible to establish a unique and straightforward correlation between K_h and soil stiffness E. Deriving K_h of the springs from E of the continuum involves trying to establish a link between parameters of different *models*. Yet engineers are familiar with moduli E, not with K_h, and many times even crude relations E to K_h may prove useful.

Typical ranges of K_h can be found in the literature, but great care is required owing to the problem-dependent nature of the parameter. For a given soil, values appropriate for strips, rafts, laterally loaded piles and flexible walls are all different (Clayton et al. 1993).

3 EXISTING K_h FORMULATIONS FOR WALLS

Various methods have been proposed for evaluating K_h for retaining walls (e.g. Terzaghi 1955, Ménard et al. 1964, Balay 1984, Becci & Nova 1987, Schmitt 1995, Simon 1995). Most formulations assume that K_h [F·L^{-3}] is directly proportional to the soil modulus E [F·L^{-2}]. In essence, almost all studies arrive to similar conversion

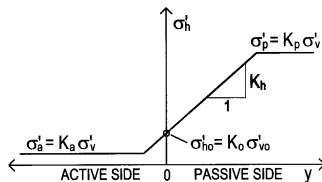
Fig. 1. Typical pressure-displacement relation of the springs

formulae $K_h \sim E/B$, where B is a dimension [L] which represents the width of the soil area "loaded" by the wall.

Most existing methods give indications for evaluating B for the simple mechanism of cantilever wall, generally suggesting to assume B proportional to the free cantilever height or embedded length. The behavior of multi-restrained walls is more complex and the estimate of B is uncertain, since the earth pressure distribution and the mode of deformation of the wall are not known *a priori*. E.g. multi-propped thick concrete diaphragm walls constructed by top-down technique, with basement floor slabs used as struts, generally exhibit a very stiff "box-type" behavior. The earth pressure may remain close to K_0 and multiple restraints permit only very small wall displacements. Hence K_h (ratio pressure/displacement) is ex-

pected to be higher, i.e. B lower, than for cantilever walls. FEM studies on propped and cantilever walls by Potts & Fourie (1984, 1986) and Fourie & Potts (1989) pointed out the enormous importance of the mode of deformation and displacement restraint on the earth pressure distribution and the resultant wall bending moments.

Various contributions on K_h given by French researchers are based on the original method by Ménard et al. (1964), which derives K_h over the embedded length of a cantilever wall from the pressuremeter modulus E_M:

$$K_h = E_M / [\alpha \cdot a/2 + 0.13 (9\, a)^{\alpha}] \qquad (1)$$

This formula contains a dimensional parameter a (in m) related to wall geometry and a non dimensional factor α related to soil type. Ménard et al. (1964) assumed $a = 2/3$ of the embedded wall length ($\approx$ distance between bottom of excavation and center of rotation at the toe of the wall). In practice a = height over which the soil is loaded by passive pressure. (Similar indications were given by Terzaghi 1955).

As reported by Amar et al. (1991), the pressuremeter modulus E_M is related to the oedometer modulus (in the same range of pressure) by the ratio $E_{oed} = E_M / \alpha$. For NC soils α varies between 1/3 in sands to 2/3 in clays (Ménard & Rousseau 1962). In principle, M_{DMT} (1-D modulus from DMT) can be used in Eq. 1 or derived formulae in place of E_M / α. (Various studies, e.g. Kalteziotis et al. 1991, Ortigao et al. 1996, Brown & Vinson 1998, have quoted similar ratios - generally $\approx$ 1/2 - between PMT and DMT moduli in different soils).

Balay (1984) adapted the Ménard formulation for evaluating K_h over the entire wall length, assuming a = H (free cantilever height) above excavation level, while below the excavation a is related to the embedded length D and to the ratio D/H.

Schmitt (1995), based on the observation of different modes of deformation of stiff and flexible walls, adapted the Ménard formulation to take into account the flexural inertia of the wall EI, assuming $a \sim (EI/E_{oed})^{0.33}$ and $E_{oed} = E_M/\alpha$, thus obtaining:

$$K_h = 2.1\,(E_{oed}^{4/3} / EI^{1/3}) \qquad (2)$$

According to the above relation, for a given soil modulus a stiff wall would have a lower K_h than a flexible wall. (Earlier studies on spread footings had indicated a lower influence of structure stiffness on K, e.g. Vesic 1961 found K inversely proportional to $EI^{1/12}$).

Simon (1995) extended the Ménard formulation adapted by Balay (1984) differentiating K_h for zones of "free" deformations (free height and embedded length of cantilever wall) and "restrained" deformations (zones between two props/anchors and behind

a pretensioned anchor). For the zone between two props at distance L, assuming that a foundation of width B causes deformations over a length $L \approx 1.5\,B$, Simon (1995) proposed:

$$K_h = E_M / [0.13\,(4.4\,B)^{\alpha} + \alpha \cdot B/6] \tag{3}$$

The method by Becci & Nova (1987) differs from other spring methods for taking into account the non linear soil behavior, assuming the soil modulus E varying with stress level and loading path direction. K_h is evaluated as:

$$K_h = a \cdot E / L \tag{4}$$

E is assumed as the unloading-reloading modulus E_{ur} where the present stress level is lower than the maximum past stress level, as the virgin compression modulus when the maximum past stresses are exceeded. a is a non dimensional empirical factor (the Authors assume $a = 1$). As first approximation, L ($\approx$ width of soil zone involved by the wall movement) is assumed as an "average" width of the Rankine active and passive pressure wedges behind and in front of the wall (this leads to different K_h on the two sides).

4 FEM INPUT PARAMETERS

The geometry of the multi-propped wall selected for this study (Fig. 2) reproduces a typical configuration of common excavation works (e.g. car parking with 6 basement floors). The final depth of the excavation is 18 m. The total length of the wall is 24 m (embedded length 6 m). Six prop levels are equally spaced at 3 m intervals. The upper prop level is placed just at the top of the wall (ground surface). The half-width of the excavation is 20 m.

The finite element mesh used in Plaxis (plane strain analysis) is shown in Fig. 3. The wall was schematized as a "beam" element. The props were simulated by Plaxis "fixed-end anchor" elements (elastic springs of given axial stiffness, having one "movable" end connected to the wall and the other end "fixed" - zero displacement - at given longitudinal distance from the wall).
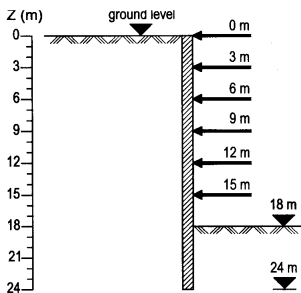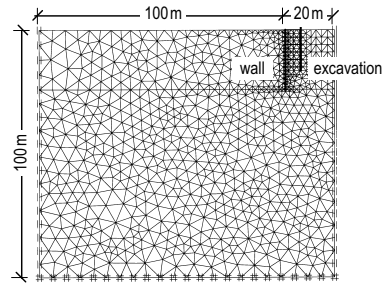

Fig. 2. Geometry of multi-propped wall

Fig. 3. Finite element mesh for multi-propped wall study

The soil behavior was simulated using the non linear Hardening Soil (HS) model of the Plaxis code. This model requires to input three stiffness moduli at the reference pressure $p^{ref} = 100$ kPa: the tangent oedometer modulus E_{oed}^{ref}, the triaxial modulus E_{50}^{ref}, the unloading- reloading modulus E_{ur}^{ref}. All moduli are stress-level dependent, according to the expressions $E_{oed} = E_{oed}^{ref} (\sigma'_1 / p^{ref})^m$, $E_{50} = E_{50}^{ref} (\sigma'_3 / p^{ref})^m$, $E_{ur} = E_{ur}^{ref} (\sigma'_3 / p^{ref})^m$, where σ'_1 and σ'_3 are the major and minor principal effective stresses. (Usually $m \approx 0.5$ to 1).

An intensive literature survey by Schanz & Vermeer (1997) indicated for remolded quartz sands (from very loose silty sands to very dense gravelly sands) $E_{50}^{ref} = 15$ to 75 MPa. The above range is remarkably similar to the range of M_{DMT} values found for sands of similar density. Schanz & Vermeer (1997) showed that E_{50}^{ref} is correlated to the 1-D modulus E_{oed}^{ref}. Hence, if one has data on the oedometer modulus, it can be used to estimate the triaxial modulus. Based on the above considerations, in this study it was assumed $E_{oed} = M_{DMT}$, and all moduli required by the Plaxis HS model were estimated assuming M_{DMT} as the basic reference stiffness parameter. According to indications given by Plaxis researchers (Vermeer 2001), the following "typical" ratios between different moduli were adopted: $E_{50}^{ref} = E_{oed}^{ref}$, $E_{ur}^{ref} = 4\,E_{oed}^{ref}$.

Two soil types were considered: a "soft soil" (e.g. a soft to medium clay) having $M_{DMT} = 4$ MPa and a "stiff soil" (e.g. a hard clay or a medium dense sand) having $M_{DMT} = 40$ MPa (at $p^{ref} = 100$ kPa). The above M_{DMT} values were selected to generally characterize a wide category of soft and stiff soils, and do not refer to any particular site. Having a real M_{DMT} profile from a specific site for a homogeneous soil, one could assume $E_{oed}^{ref} = M_{DMT}$ at $\sigma'_v = 100$ kPa. Also, the exponent m could be inferred from the rate of increase of M_{DMT} with depth.

The only difference between the "soft soil" and the "stiff soil" relates to stiffness. The "stiff soil" is simply a factor 10 stiffer than the "soft soil", but the relation $E_{50}/E_{oed}/E_{ur}$ is 1/1/4 for both soils. For both soils it was assumed $m = 0.5$ and $\nu_{ur} = 0.2$ (Poisson's ratio for unloading-reloading). All other parameters, in particular shear strength, were conveniently as-

sumed equal for both soils: bulk unit weight γ = 19 kN/m^3, friction angle Φ' = 30°, dilatancy angle ψ = 0, cohesion c' = 0.5 kPa, wall/soil friction angle δ = 20°. The wall was assumed to be installed without altering the in situ conditions ("wished in place"). The initial stresses were calculated assuming K_0 = 0.5.

The present study is restricted to fully drained conditions, with zero pore pressures everywhere. Seepage pressures have been ignored at this stage of the study, in an attempt to investigate the effects of earth pressures alone on the wall behavior.

Four different soil / wall stiffness combinations were considered (Table 1). The "rigid wall" is a 1 m thick reinforced concrete diaphragm wall, having Young's modulus E = 25000 MPa. The "flexible wall" is a steel sheetpile wall of similar structural capacity. Note that Case A and Case D have similar wall/soil stiffness ratios ($EI/E_{oed}{}^{ref}$ = 58 and 52 respectively). For Case B $EI/E_{oed}{}^{ref}$ = 521. For Case C $EI/E_{oed}{}^{ref}$ = 5.8. Hence the wall/soil stiffness relation between the various cases is $\approx$ 1/10/100.

Very stiff props (30 cm thick concrete slabs, axial stiffness EA = 7500 MN/m) are associated to the "rigid wall" scheme. The "flexible wall" is supported by steel props of lower stiffness (EA = 657 MN/m). No prestress force was given to the props. The excavation sequence was simulated assuming that each prop level, starting from the uppermost one, is installed before excavating the 3 m soil layer immediately below, down to the next prop level (as in the top-down technique).

5 FEM RESULTS FOR MULTI-PROPPED WALL

The results of Plaxis analyses obtained for Cases A, B, C and D at the maximum excavation depth (18 m) are summarized in Fig. 4. Observations:
(a) The horizontal effective stresses developed on the back and on the front of the wall resulting from Plaxis calculation are shown in Fig. 4, compared to the distributions of at-rest, active and passive earth pressures (K_a and K_p calculated according to Caquot & Kerisel 1948). In general the full active condition behind the wall is not reached and σ'_h is intermediate between the initial K_0 and the K_a line. The passive pressure K_p is mobilized over $\approx$ 1/3 of the embedded wall length. Note that the earth pressure distribution is quite similar for Cases A and D, having similar wall/soil stiffness ratios.
(b) An "anomalous" earth pressure distribution results from the combination stiff soil/flexible wall (Case C). The progressive deflections of the wall towards the excavation promote the redistribution of σ'_h behind the wall in the embedded length and upper restrained zones (arching), while just above excavation level σ'_h decreases even below the

"theoretical" minimum K_a. The maximum bending moment is much smaller than in all other cases, less than 50 % of the value calculated for the same soil in combination with the "rigid wall". A significant "fixity" moment at the toe of the wall is also observed in this case. (Similar results were obtained by Vermeer 2001 for a single-anchored wall of similar EI/E_{oed} ratio)
(c) The maximum horizontal displacements occur at $\approx$ 15-18 m depth, near the bottom of the excavation. The top of the wall does not move at all, due to the restraint provided by the upper props. This "deep" mode of deformation is opposite to the cantilever-type.
(d) The diagrams on the right in Fig. 4, inferred from Plaxis results, represent the variation of the earth pressure σ'_h on the back of the wall vs the horizontal wall displacement y at various depths (each curve refers to a given depth z, at 1.5 m intervals). To compare curves obtained at different depths, σ'_h is normalized to the vertical stress (earth pressure coefficient $K = \sigma'_h / \sigma'_v$) and the horizontal displacement y is normalized to depth z (ratio y/z). The dashed horizontal lines represent the at-rest (initial) K_0 and the active K_a pressure coefficients. These curves correspond to the "active side" of the spring pressure-displacement curve in Fig. 1. (The attention is focused here on the "active side", more significant than the "passive side" for multi-propped walls, since their embedded length is generally small compared to the retained height). The figures show that, as the wall moves towards the excavation, σ'_h behind the wall varies differently from one case to another. In general K_a is not reached, except for Case C. In Cases A, C and D, after an initial decrease, σ'_h tends even to increase (well beyond K_0 in Case C) with wall displacement. (Again, the curves obtained for Cases A and D are quite similar). Only in Case B σ'_h decreases continuously. In general, however, the slope of the "normalized" curves obtained at various depths for each case is similar. Since the slope of these curves is equal to K_h of the springs ($K_h = \Delta\sigma'_h / \Delta y$) divided by the unit weight γ (assumed constant), this suggests that adopting K_h constant with depth in spring calculations should not involve a large error, at least as first approximation.

Table 1. Soil and wall stiffness parameters

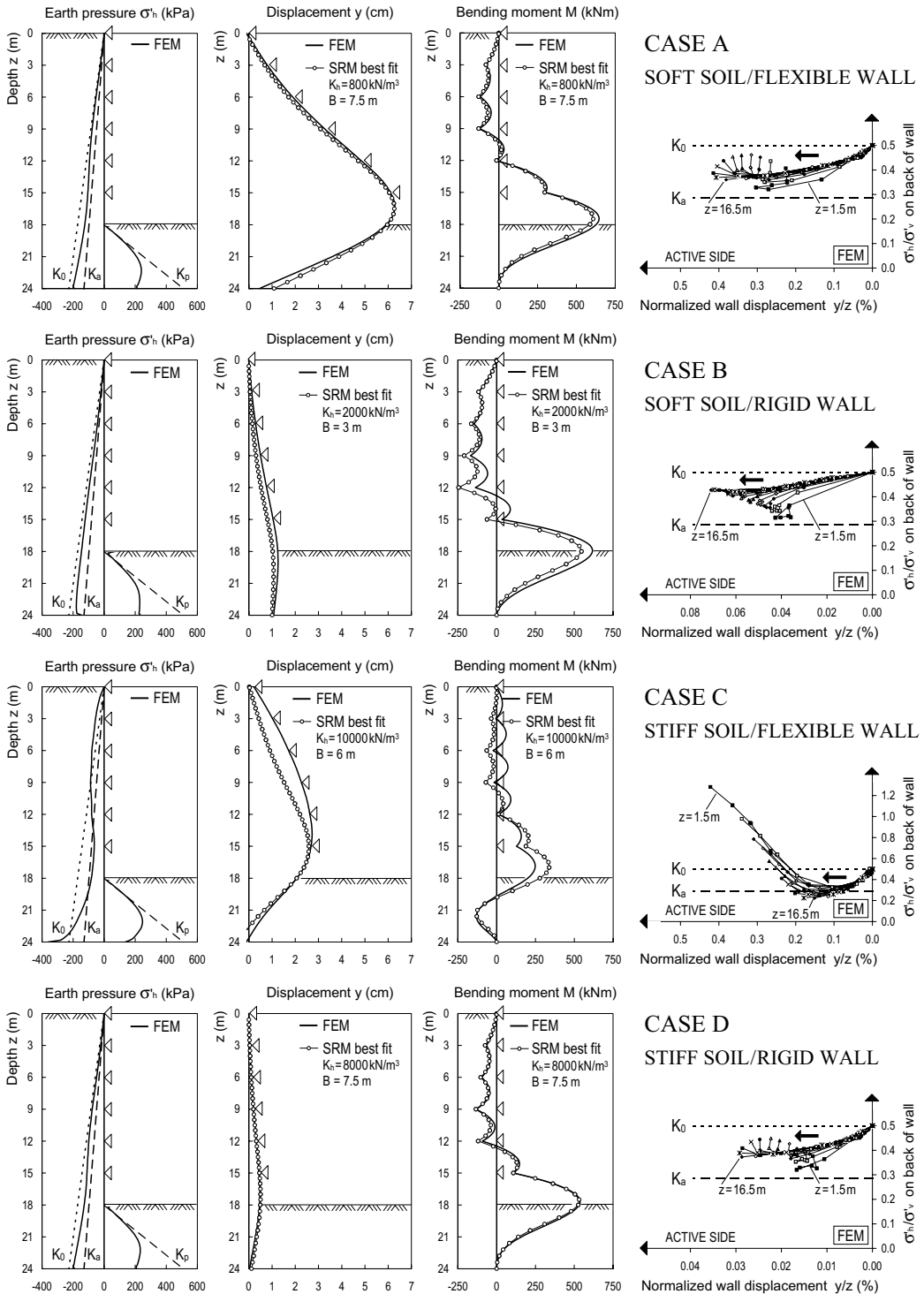|	Soil stiffness $E_{oed}{}^{ref}$ (MPa)	Wall stiffness EI (MNm^2/m)
Case A soft soil/flexible wall	4	232
Case B soft soil/rigid wall	4	2083
Case C stiff soil/flexible wall	40	232
Case D stiff soil/rigid wall	40	2083

Fig. 4. Results of FEM and SRM analyses for multi-propped wall. Earth pressure distribution, horizontal wall displacements and bending moments at 18 m excavation depth. Normalized pressure–displacement curves on back of wall at 1.5 m depth intervals.

6 SPRING ANALYSIS RESULTS

The Subgrade Reaction Method was used to simulate the behavior of the multi-propped wall in Fig. 2, considering the same four cases analyzed by FEM. For each case SRM calculations were repeated varying Kh until the bending moments and the horizontal displacements of the wall were nearly equal to the values calculated by Plaxis.

As first approximation, K_h were assumed constant with depth and through all calculation steps, and equal on both sides of the wall. (A better estimate would involve K_h varying with depth and calculation sequence, e.g. K_h decreasing as excavation depth increases, and possibly different on the active and passive side).

The profiles of the horizontal displacements and bending moments calculated by SRM for the "best fit" K_h, i.e. the K_h values for which SRM results "match" FEM results (assuming the bending moment as "target" parameter), are shown in Fig. 4, superimposed to the Plaxis results. (The "best fit" K_h for matching horizontal displacements may differ slightly). Observations:

(a) The SRM reproduces well Plaxis results in Cases A and D, of "intermediate" wall/soil stiffness. The ratio between the "best fit" K_h calculated for the above two cases ($K_h = 800$ and 8000 kN/m^3 respectively) is equal to the ratio between the corresponding soft/stiff soil moduli (1/10), confirming K_h proportional to soil stiffness.

(b) For Cases B and C, of "high" and "low" wall/soil stiffness respectively, the SRM is not able to reproduce Plaxis results with the same accuracy, even adopting different distributions of K_h with depth. This result is presumably a consequence of the limited ability of the spring model to simulate the soil behavior in particular conditions (e.g. in Case C arching cannot be simulated, since the spring would yield plastically as soon as K_a is reached and the earth pressure will never reach smaller values). The "best fit" backcalculated values are $K_h = 2000$ kN/m^3 for Case B, $K_h = 10000$ kN/m^3 for Case C.

The axial forces in the props calculated for the "best fit" K_h are generally in good agreement (± 10-20%) with the values calculated by Plaxis. Only in Case C the SRM largely underestimates (-40-60%) the forces in the upper prop levels.

The "best fit" K_h backcalculated from Plaxis results were compared to the values determined by various existing K_h formulations. The range of K_h obtained according to Eq. 4 by Becci & Nova (1987), assuming E = virgin compression modulus (not varying with stress, as first approximation), is similar to the "best fit" K_h. Also the K_h obtained according to Balay (1984) are not so far from the "best fit" K_h. The formulation by Schmitt (1995) overestimates K_h, giving K_h for the "rigid wall" less than 50 % of K_h for the "flexible wall", in contrast with the results of SRM-FEM comparison. The K_h obtained according to the formula by Simon (1995) for the inter-prop zone are also overestimated.

Hence, for the examined cases, existing K_h formulations taking into account wall/soil stiffness and restraint conditions do not reproduce the FEM-calculated behavior better than methods which do not take into account the above factors.

7 INFLUENCE OF EXCAVATION DEPTH AND PROP SPACING ON K_h

In order to investigate the influence of the excavation depth on K_h, FEM and SRM calculations for the multi-propped wall were repeated considering two different excavation depths, $H = 12$ m and $H = 24$ m. In both cases the embedded wall length was assumed equal to 6 m, as in the 18 m excavation previously considered.

For each excavation depth ($H = 12$, 18 and 24 m) the calculation was repeated assuming two different values of prop spacing, $s = 3$ m and $s = 6$ m.

This analysis was carried out only for the "rigid wall" (1 m thick concrete diaphragm wall).

Besides the "soft" and the "stiff" soil ($E_{oed}^{ref} = 4$ and 40 MPa respectively), a soil of "intermediate" stiffness ($E_{oed}^{ref} = 16$ MPa) was also considered. The above values of E_{oed}^{ref}, relative to a reference pressure $p^{ref} = 100$ kPa, correspond to average values of the constrained modulus M_{DMT} over the entire wall length equal to $M_{DMT} \approx 5$-7 MPa for the "soft" soil, $M_{DMT} \approx 20$-30 MPa for the "intermediate" soil and $M_{DMT} \approx 50$-70 MPa for the "stiff" soil.

The "best fit" K_h resulting from SRM-FEM comparison for the examined cases are shown in Figs. 5 and 6. Fig. 5 shows that, for given soil stiffness M_{DMT} (average over total wall length) and prop spacing, K_h decreases significantly as the excavation depth increases from 12 to 18 m, but remains practically unchanged from 18 to 24 m. For given M_{DMT} and excavation depth, K_h decreases as prop spacing increases from 3 to 6 m, but such reduction is more pronounced for the lower depth ($H = 12$ m). In essence, K_h decreases as excavation depth and prop spacing increase, but the influence of both factors on K_h is smaller at higher excavation depths.

Fig. 6 shows the variation of K_h with M_{DMT} (average over total wall length) for different values of excavation depth and prop spacing. K_h increases with M_{DMT}, as expected. In most cases, for a given value of M_{DMT}, the values of K_h vary over a relative narrow range. Only in the case $H = 12$ m and $s = 3$ m (a nearly "zero displacement" restraint condition) K_h is significantly higher.
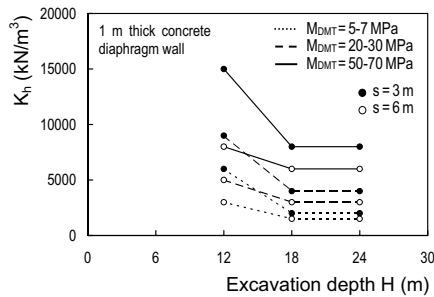
Fig. 5. "Best fit" K_h vs excavation depth H for different values of constrained soil modulus M_{DMT} and prop spacing s
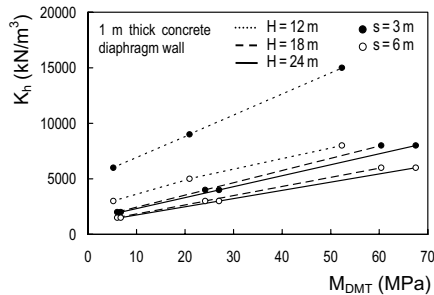

Fig. 6. "Best fit" K_h vs constrained soil modulus M_{DMT} for different values of excavation depth H and prop spacing s

8 TENTATIVE CORRELATION $K_h - M_{DMT}$

The results obtained for the examined cases indicate that K_h tends to decrease when the wall is subject to larger deformations as a consequence of deeper excavation or lower restraint degree, i.e. the width B of the soil zone involved by the wall movement increases. An attempt was made to interpret the above results based on a simple relation between K_h and the constrained soil modulus M_{DMT}, having the form (similar to existing K_h formulations):

$$K_h = M_{DMT}/B \qquad (5)$$

The values of the "characteristic length" B obtained from Eq. 5 for the "best fit" K_h are plotted in Fig. 7 vs excavation depth, for three different ranges of M_{DMT} (average over total wall length) and two values of prop spacing ($s = 3$ m and $s = 6$ m). For a given M_{DMT}, B increases as excavation depth and prop spacing increase. For given excavation depth and prop spacing, B increases with M_{DMT}. For a "typical" wall configuration, say excavation depth $H = 18$ m and prop spacing $s = 3$ m, $B = 3$ m for $M_{DMT} = 5$-7 MPa, $B = 6$ m for $M_{DMT} = 20$-30 MPa, $B = 7.5$ m for $M_{DMT} = 50$-70 MPa. (The B values calculated for $H = 18$ m for Cases A, B, C and D are indicated in Fig. 4).

Fig. 7 may be used as a broad indication for se-

lecting the values of B - hence K_h - for design of multi-propped diaphragm walls in cases of similar wall geometry / stiffness and prop spacing for different ranges of M_{DMT}.

For multi-propped walls it appears logical to link B to the retained excavation height H, not to the total or embedded length of the wall. In fact in this case, unlike for cantilever walls, the embedded length has a minor influence on the wall behavior and its value is not strictly dependent on wall equilibrium considerations. In the examined cases the ratio B / H was found ≈ 0.1-0.2 for $M_{DMT} = 5$-7 MPa, 0.2-0.4 for $M_{DMT} = 20$-30 MPa and 0.3-0.6 for $M_{DMT} = 50$-70 MPa.

9 COMPARISON WITH CANTILEVER WALL

To investigate the influence of restraints on K_h, the behavior of the "highly-restrained" multi-propped wall was compared to the behavior of a "fully-unrestrained" cantilever wall. FEM and SRM analyses were carried out for Cases A, B, C and D (Fig. 8), considering an excavation of 8 m depth. The embedded wall length (8 m) was established based on a conventional limit equilibrium analysis, assuming a factor of safety $Fs = 1.5$ on K_p. The excavation was simulated by 8 steps, each one corresponding to a 1 m excavation, to investigate in detail the initial part of the pressure-displacement curves. Observations:

(a) The full K_a condition is reached behind a large part of the wall in all cases, as expected, while σ'_h increases rapidly near the toe. K_p is mobilized over $\approx 1/4$ of the embedded length. This earth pressure distribution is consistent with the presence of a point of rotation at ≈ 6-6.5 m depth below excavation level.

(b) The "best fit" backcalculated values ($K_h = 800$-900 kN/m^3 for the "soft soil", $K_h = 8000$-10000 kN/m^3 for the "stiff soil") confirm the linear relation between K_h and soil modulus. For cantilever walls, the wall / soil stiffness has a minor influence on K_h. (In this case the "target" parameter of the SRM-FEM comparison was the wall displacement, since, as well known, for a cantilever wall the bending moments are practically not influenced by K_h).

(c) The K_h obtained for the cantilever wall for an excavation of 8 m depth are similar to the K_h found for the multi-propped wall for an excavation of 18-24 m depth.

(d) The "characteristic length" calculated based on Eq. 5 is $B \approx 5$-6 m, i.e. $\approx 2/3$-3/4 of the embedded length, very close to the values indicated by earlier K_h methods (e.g. Ménard et al. 1964). For cantilever walls, it appears appropriate to link B to the embedded wall length.

(e) The "normalized" pressure–displacement curves behind the wall at various depths (at 1 m intervals) calculated by Plaxis for the cantilever wall

are significantly different from those obtained for the multi-propped wall (Fig. 4). σ'_h behind the wall decreases as wall displacement increases, and remains constant after K_a is reached. The initial part of the curves (shown in Fig. 8) is remarkably non linear. This behavior could be more closely simulated assuming for the springs a non linear pressure-displacement relation (e.g. similar to existing DMT-based formulations of P–y curves for laterally loaded piles by Robertson et al. 1987, Marchetti et al. 1991), instead of the classical bilinear relation in Fig. 1. It is questionable, however, that this would lead to a substantially more accurate prediction of wall behavior, in view of the intrinsic approximation involved by the spring approach.

10 CONCLUSIONS

The Subgrade Reaction Method is widely used in current practice for design of multi-propped walls. Of course the crucial step is the selection of an appropriate value of the coefficient of subgrade reaction K_h. The numerical study illustrated in this paper investigates the influence of various factors on K_h (soil and wall stiffness, excavation depth, prop spacing). The possible K_h-DMT relationship is "calibrated" based on the results of FEM analyses carried out using the non linear Plaxis Hardening Soil model.

Several comparisons of DMT moduli vs "reference" moduli and DMT-predicted vs measured settlements (see e.g. TC16 2001) have shown that, in general, the constrained modulus M from DMT is a reasonably accurate "operative" modulus. Schanz & Vermeer (1997) indicated, for very loose to very dense sands, a range of values of the triaxial modulus E_{50}^{ref} (basic input parameter of Plaxis HS model, correlated to the 1-D modulus E_{oed}^{ref}) very similar to the range of M_{DMT} found for sands of similar density. In this study it was assumed $E_{oed} = M_{DMT}$, and all moduli required by the HS model were estimated assuming M_{DMT} as the basic reference stiffness parameter.

The results presented in this paper, though relative to a limited number of cases, indicate that K_h is proportional to soil stiffness and decreases as excavation depth and prop spacing increase, but its value tends to remain constant after a certain excavation depth is exceeded. The wall / soil stiffness largely influences the earth pressure distribution on the wall, but has a lower influence on K_h.

A tentative correlation between K_h and M_{DMT} is proposed, having the form $K_h = M_{DMT} / B$. Fig. 7 may be used as a broad indication for selecting the values of B - hence K_h - for design of multi-propped diaphragm walls in cases of similar wall geometry / stiffness and prop spacing for different ranges of M_{DMT}.

The B values ($B \approx 3$ to 8 m) obtained for "typical" multi-propped wall configurations (excavation depth 18-24 m, prop spacing 3 m) are similar to the values ($B \approx 5$-6 m) found for a cantilever wall for excavation depth 8 m.

Further investigations are needed to take into account different conditions and additional factors which may influence K_h (e.g. seepage pore pressures), in order to obtain indications for the selection of K_h in the general case.

Of course the results of this numerical study need to be validated based on field data from real cases.
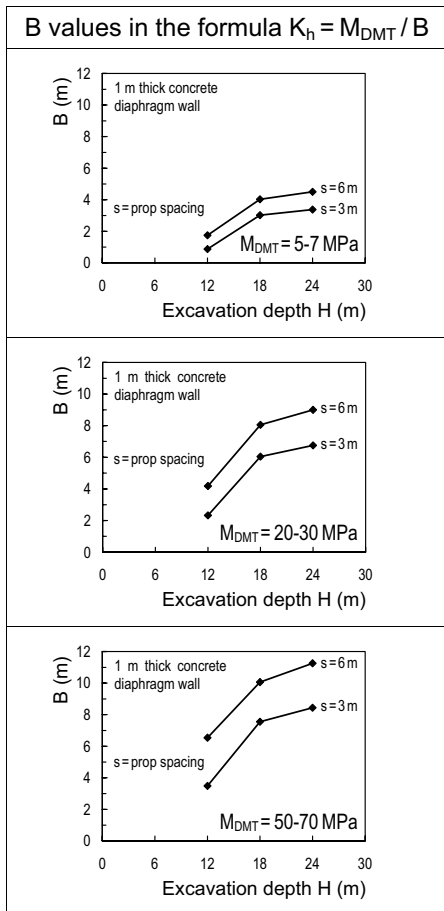

Fig. 7. Characteristic length B (M_{DMT} / K_h) vs excavation depth H for different values of M_{DMT} (average over total wall length) and prop spacing s
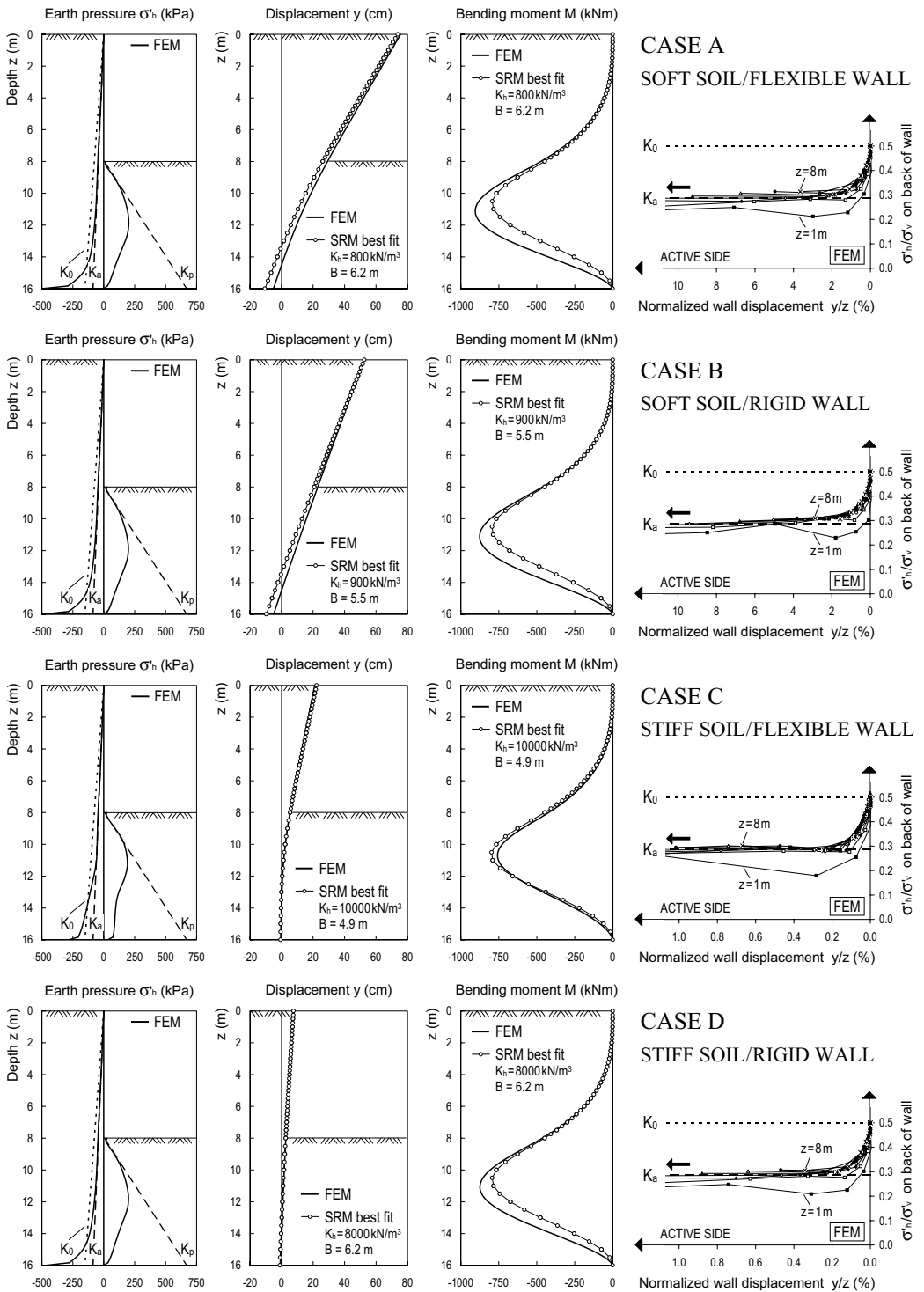
Fig. 8. Results of FEM and SRM analyses for cantilever wall. Earth pressure distribution, horizontal wall displacements and bending moments at 8 m excavation depth. Normalized pressure–displacement curves on back of wall at 1 m depth intervals.

REFERENCES

Amar, S., Clarke, B.G.F., Gambin, M.P. & Orr, T.L.L. 1991. The application of pressuremeter test results to foundation design in Europe. A state-of-the-art report by the ISSMFE European Technical Committee on Pressuremeters. Part 1: Predrilled pressuremeters and self-boring pressuremeters. A.A. Balkema.

Balay, J. 1984. Recommandations pour le choix des paramètres de calcul des écrans de soutènement par la méthode aux modules de réaction. *Note d'Information Technique, Laboratoire Central des Ponts et Chaussées*.

Becci, B. & Nova, R. 1987. Un metodo di calcolo automatico per il progetto di paratie. *Rivista Italiana di Geotecnica* 21, 1: 33-47.

Brown, D.A. & Vinson, J. 1998. Comparison of strength and stiffness parameters for a Piedmont residual soil. *Proc. 1st Int. Conf. on Site Characterization ISC'98, Atlanta,* 2: 1229-1234.

Caquot, A. & Kerisel, J. 1948. Tables for the Calculation of Passive Pressure, Active Pressure and Bearing Capacity of Foundations. Gautiers-Villars, Paris.

Clayton, C.R.I., Milititsky, J. & Woods, R.I. 1993. Earth pressure and Earth-retaining Structures. Chapman & Hall.

Fourie, A.B. & Potts, D.M. 1989. Comparison of finite element and limiting equilibrium analyses for an embedded cantilever retaining wall. *Géotechnique* 39, 2: 175-188.

Kalteziotis, N.A., Pachakis, M.D. & Zervogiannis, H.S. 1991. Applications of the Flat Dilatometer Test (DMT) in Cohesive Soils. *Proc. X ECSMFE, Florence,* 1: 125-128.

Marchetti, S. 1980. In Situ Tests by Flat Dilatometer. *ASCE Jnl GED*, 106, GT3: 299-321.

Marchetti, S., Totani, G., Calabrese, M. & Monaco, P. 1991. P-y curves from DMT data for piles driven in clay. *Proc. 4th DFI Int. Conf. Piling and Deep Foundations, Stresa,* 1: 263-272.

Ménard, L., Bourdon, G. & Houy, A. 1964. Étude expérimentale de l'encastrement d'un rideau en fonction des caractéristiques pressiométriques du sol de fondation. *Sols Soils* 9.

Ménard, L. & Rousseau, J. 1962. L'évaluation des tassements, tendances nouvelles. *Sols Soils* 1.

Ortigao, J.A.R., Cunha, R.P. & Alves, L.S. 1996. In situ tests in Brasilia porous clay. *Canad. Geot. Jnl*, 33, 1: 189-198.

Potts, D.M. & Fourie, A.B. 1984. The behaviour of a propped retaining wall: results of a numerical experiment. *Géotechnique* 34, 3: 383-404.

Potts, D.M. & Fourie, A.B. 1986. A numerical study of the effects of wall deformation on earth pressures. *Int. Jnl for Num. and Analytical Methods in Geomech.* 10: 383-405.

Robertson, P.K., Davies, M.P. & Campanella, R.G. 1987. Design of Laterally Loaded Driven Piles Using the Flat Dilatometer. *Geot. Testing Jnl*, 12, 1: 30-38.

Schanz, T. & Vermeer, P.A. (1997). On the Stiffness of Sands. *Proc. Symp. Pre-failure Deformation Behaviour of Geomaterials, ICE, London*: 383-387.

Schmitt, P. 1995. Méthode empirique d'évaluation du coefficient de réaction du sol vis-à-vis des ouvrages de soutènement souples. *Revue Française de Géotechnique* 71: 3-10.

Simon, B. 1995. Commentaires sur le choix des coefficients de réaction pour le calcul des écrans de soutènement. *Revue Française de Géotechnique* 71: 11-19.

TC16. 2001. The Flat Dilatometer Test (DMT) in Soil Investigations - A Report by the ISSMGE Committee TC16.

Terzaghi, K. 1955. Evaluation of coefficients of subgrade reaction. *Géotechnique* 4: 297-326.

Vermeer, P.A. 2001. On single anchored retaining walls. *Plaxis Bulletin* 10.

Vesic, A.B. 1961. Bending of beams resting on isotropic elastic solid. *ASCE Jnl Engineering Mech. Div.* 87, EM2: 35-53.